Composites Science and Technology 94 (2014) 105–110

Contents lists available at ScienceDirect

Composites Science and Technology

journal homepage: www.elsevier.com/locate/compscitech

Preparation of UV-curable transparent poly(urethane acrylate) nanocomposites with excellent UV/IR shielding properties

Haifeng Zhou, Hua Wang, Xingyou Tian *, Kang Zheng, Zhaofeng Wu, Xin Ding, Xianzhu Ye

Key Laboratory of Materials Physics, Institute of Solid State Physics, Chinese Academy of Sciences, Hefei 230031, China

ARTICLE INFO

Article history:
Received 15 October 2013
Received in revised form 20 January 2014
Accepted 28 January 2014
Available online 4 February 2014

Keywords:
A. Nanocomposites
A. Functional composites
B. Optical properties

ABSTRACT

Due to the great potential applications, high transparent organic–inorganic nanocomposites have attracted wide attention over past decade. However, it is still a challenge to maintain the transparency of optical materials due to the light scattering caused by the severely aggregation of nanoparticles (NPs) when they are introduced into the polymer matrix. In this report, we describe the preparation of UV-curable transparent poly(urethane acrylate) (PUA) nanocomposites with 3-(trimethoxysilyl)propyl-methacrylate (MPS) modified ITO NPs. The FTIR and TGA results confirmed that the MPS was grafted to the surface of ITO NPs successfully. It was found that the incorporation of ITO NPs not only provided UV shielding ability to the nanocomposite coatings with the similar transparency of the pure PUA, but also exhibited low transmittance of near-infrared (NIR) light. And, the cutoff wavelength of the composites in NIR range (800–2500 nm) shifts toward the lower wavelength as ITO concentration increasing. The transmittance of the nanocomposite coatings with 0 wt.%, 1 wt.%, 3 wt.%, 5 wt.%, 7 wt.% and 9 wt.% of the ITO NPs at 1500 nm in the NIR region are 91%, 56%, 38%, 31%, 18% and 6%, respectively.

1. Introduction

With increasing environmental and energy saving concern, extensive researches have focused on the development of inorganic–polymer nanocomposites that present high visible wavelength transparency as well as high UV/infrared (IR) shielding properties [1–11]. This class of polymer–inorganic functional materials can be fabricated by incorporating transparent conducting oxides (TCOs) NPs into a transparent polymeric matrix and are ideal for applications such as UV/IR shielding windows in automobiles and buildings, contact lenses, and optical filters. TCOs, typically wide bandgap oxide semiconductors such as aluminum-doped zinc oxide, antimony-doped tin oxide, tin-doped indium oxide (ITO), exhibit the good combination of high transmittance in the visible region and low transmittance in the infrared region of light [12–14]. Among these, ITO is attractive due to its remarkable optical properties and high thermal stability [15,16]. UV-radiation curing has attracted great interests and become commercially important in wide applications because of the rapid ambient crosslinking, solvent free characteristics and low energy requirements [17–19]. Also, it has been extensively and successfully applied in the production of polymer composites during the past decade.

Many works have been done to fabricate the ITO/polymer nanocomposites and investigate the optical properties. For example, Miyazaki et al. [7] synthesized transparent ITO/polymer materials by simple blending of ITO NPs with urethane resin, and found that a mixing ratio composite of 1.0 vol% of ITO NPs was not transparent in the IR wavelength region while the transmittance in the visible wavelength region was under 40%. Capozzi and Gerhardt [20] prepared the PMMA/ITO nanocomposites by mechanical mixing and compression molding, and the UV–VIS spectrophotometry analysis indicated that the nanocomposites completely lost their optical transparency with 3 wt.% loading of ITO NPs. The serious transmittance loss in visible wavelength region of the two above mentioned ITO/polymer nanocomposites are related to the intense light scattering caused by the agglomeration of the NPs in the polymer matrixes. Thus, to fabricate a highly transparent ITO/polymer nanocomposite, it is crucial to have the uniform dispersion of ITO NPs within the polymer matrix. Methods aiming to improve the dispersion of ITO NPs in the polymer matrix are of great importance to prepare high transparent UV/IR shielding materials [2,9,21,22]. For instance, Wu et al. [4] reported that the UV-curable ITO/polymer nanocomposite was synthesized by mixing the ITO slurry with UV-curable monomers and oligomer after the nano-ITO slurry was prepared by ball milling with butyl acetate as the

* Corresponding author. Tel.: +86 5515591477; fax: +86 5515591434.
E-mail address: xytian@issp.ac.cn (X. Tian).

http://dx.doi.org/10.1016/j.compscitech.2014.01.022
0266-3538/

dispersing media. Schadler et al. [6] studied the preparation of ITO NPs by the solvothermal method, followed by the modification of ITO nanoparticles with polyglycidyl methacrylate, and finally the modified ITO NPs were dispersed in an epoxy resin to prepare nanocomposites. In another research, Zeng et al. [5] fabricated transparent ITO/polymer nanocomposite films by two steps. Firstly, using N-methyl-pyrrolidone as the reaction solvent and surface modifier to prepare the functional monodisperse ITO NPs via a nonaqueous solvothermal method. Secondly, the nanocomposite films were obtained by a simple sol-solution mixing method. In the above three studies, the ITO NPs were modified with different organic agents and the nanocomposites showed good optical properties. However, only limited work has been performed to fabricate UV curable ITO/polymer nanocomposites with 3-(trimethoxysilyl)propylmethacrylate (MPS) grafted ITO NPs. MPS end capped with vinyl group is one of the important silane coupling agents, which has been widely used in the surface modification of inorganic particles to improve their dispersion in nanocomposites and the compatibility with organic polymers, especially for the UV cured polymer nanocomposites [23].

In this paper, visible transparent but UV- and IR-opaque ITO/PUA nanocomposites were prepared by incorporating the surface modified ITO NPs into a transparent UV curable urethane acrylate resin. Firstly, ITO NPs modified with 3-(trimethoxysilyl)propylmethacrylate (MPS) were dispersed the in 1,6-hexanediol diacrylate (HDDA). Then, ITO/PUA nanocomposites were obtained by mixing ITO dispersion with urethane acrylate resin and cured under UV ray. The modification of the ITO NPs were confirmed by Fourier Transform Infrared (FTIR), ThermoGravimetric Analysis (TGA) and Dynamic Light Scattering (DLS). The optical properties of the nanocomposites were examined by an ultraviolet–visible–near infrared (UV–VIS–NIR) spectrophotometer.

2. Experimental

2.1. Raw materials

Isophorone diisocyanate (IPDI), poly(1,6-hexyl 1,2-ethyl carbonate) diol (PHEC) (M_w = 2000), were supplied by An Li Artificial Leather Co., Ltd., Hefei, China. Dibutyltin dilaurate (DBTDL), ethanol, hydroxyethyl acrylate (HEA), 1,6-hexanediol diacrylate (HDDA) and 3-(trimethoxysilyl)propylmethacrylate (MPS) were purchased from Qiang Shen Chemical Reagent Co., Ltd., Nanjing, China. 2-Hydroxy-2-methyl-1-phenyl-1-propanone (Irgacure 1173) and 1-hydroxycyclohexyl phenyl ketone (Irgacure 184) purchased from Aldrich were used as photoinitiators. Indium Tin Oxide (ITO) was purchased from Hu Zheng Nano Technology Co., Ltd., Shanghai, China. The doping level of the antimony is 10 wt.%. The raw materials were used as received, except for the PHEC which were dried in vacuo at 100 °C for 2 h.

2.2. Preparation of urethane acrylate oligomers

Urethane acrylate oligomers were prepared according to the literature [24]. PHEC and IPDI (1:3 by mole) were added to a four-necked flask equipped with a mechanical stirrer, nitrogen inlet, condenser, and thermometer. The reaction mixture was stirred and carried out at 80 °C for 2 h under a dry nitrogen atmosphere. Upon reaching the theoretical NCO value (determined by a dibutylamine back titration method), HEA was added. After an additional 1 h of reaction below 60 °C, HEA-terminated oligomers were obtained. The completion of end capping reaction was confirmed by FTIR measurements.

2.3. Modification of ITO NPs

The ITO (15 g) was dispersed in 100 mL of ethanol and 2 g of deionized water, and then 1.5 g of MPS was added. The PH value was tuned with ammonia solution. The mixture was proceeded for 8 h by ball milling. The obtained NPs were washed for three times by centrifugation in absolute ethanol at 12,000 rpm and further dried.

2.4. Preparation of ITO/PUA nanocomposites

Firstly, the MPS modified ITO NPs were dispersed in HDDA via sonication. Then, ITO/PUA nanocomposites were prepared by mixing the HDDA solution (20 wt.%), urethane acrylate oligomers (78 wt.%), Irgacure 1173 (1 wt.%) and Irgacure 184 (1 wt.%). The resultant mixture was coated onto glass and exposed to UV radiation from a medium pressure 2 kW mercury lamp for 10 s. All the irradiation experiments have performed at ambient temperature in the presence of air. By changing the contents of ITO over the range of 0, 1, 3, 5, 7 and 9 wt.%, a series of ITO/PUA nanocomposites were prepared and coded as ITO/PUA-0, ITO/PUA-1, ITO/PUA-3, ITO/PUA-5, ITO/PUA-7 and ITO/PUA-9, respectively.

2.5. Characterization

Fourier transform infrared (FTIR) spectroscopy was performed on a spectrometer (Nexus, Nicolet). KBr disks were prepared after mixing (0.5%) each of the test samples with dry KBr. The particle size of the modified ITO was measured with a Malvern Zetasizer at 20 °C. Morphology of the nanocomposite films was observed with a scanning electron microscope (FESEM, Sirion 200 FEI) at 10 kV. The specimens were frozen in liquid nitrogen, fractured,

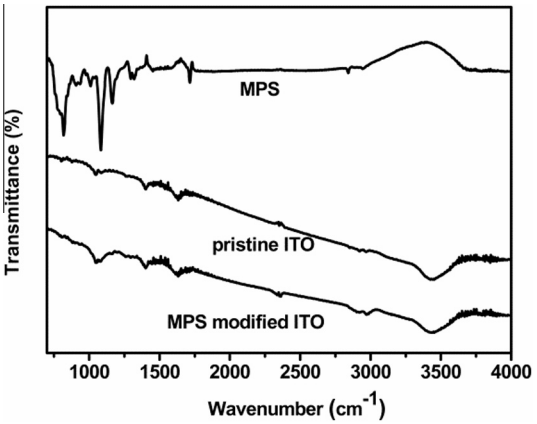

Fig. 1. FTIR spectra of MPS, pristine ITO, and MPS modified ITO NPs.

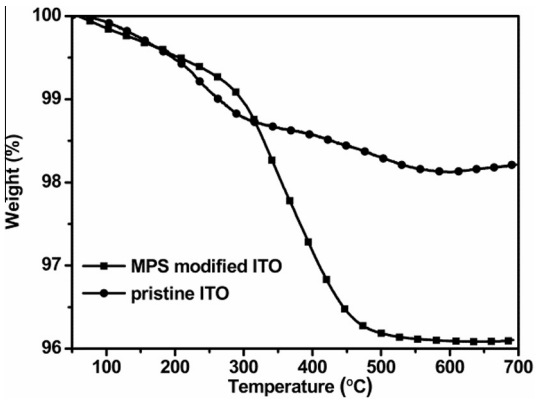

Fig. 2. TGA of pristine ITO, and MPS modified ITO NPs.

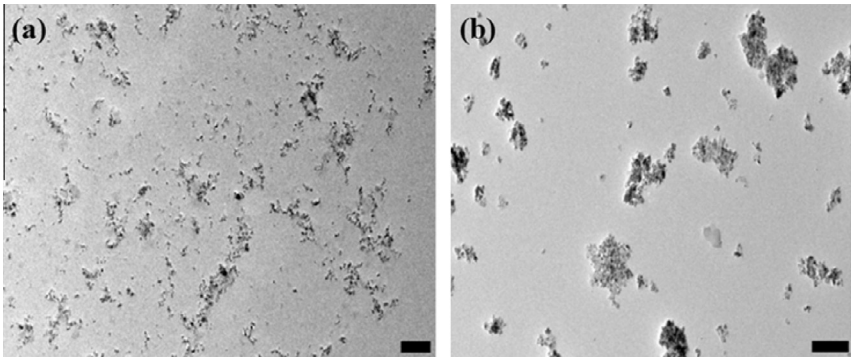

Fig. 3. TEM images of ITO NPs after (a) and before (b) modification. (Scale bars = 200 nm).

and then coated with gold. Transmission emission microscopy (JEM-2010 TEM) was used to observe the morphology of ITO NPs. The transmittance of the glass with the ITO/PUA coatings was measured by UV3600 (Shimadzu, Japan) UV–VIS–NIR spectrophotometer. The wavenumber range was set from 300 to 2500 nm.

3. Results and discussion

3.1. Surface modification of ITO NPs by MPS

MPS is one of the most efficient ligands for functionalization of inorganic oxide nanoparticles since it can react with surface hydroxyl groups of the nanoparticles in basic solution by condensation of its alkoxyl groups. Fig. 1 shows the FTIR spectra of both pristine ITO and MPS modified ITO NPs. Several absorption bands in the pristine ITO sample are considered as impurities. Apparently, most of the absorption bands of MPS modified ITO NPs are overlapped with the strong band of adsorbed impurities on the ITO. The band at 1080 cm^{-1} was corresponded to be characteristics of Si–O–C bonds in MPS, and the bands at 2901 cm^{-1} and 2969 cm^{-1} were assigned to the stretching vibration of C–H bonds of MPS. Compared to the pristine ITO, the broadened absorption band appeared at around 1080 cm^{-1}, as well as the bands at 2901 and 2969 cm^{-1} demonstrate that the condensation took place on the surface of ITO NPs. The TGA curves in Fig. 2 could be further confirmed that MPS had attached to the surface of ITO NPs. The amount of silane linked to ITO surface was about 2 wt.% which is almost comparable to the amount of the silane linked to ZnO surface (around 3 wt.%) [23]. Moreover, the sizes of the ITO particles were characterized by dynamic light scattering. The mean particle size of secondary ITO particles modified the MPS was 163 nm, while the pristine ITO particles was 313 nm which was almost two times larger than the modified ITO NPs. It is well known that the NPs tend to agglomerate due to their high surface energy. The surface modification of ITO NPs with MPS can to avoid its agglomeration effectively because of the condensation reactions between the surface hydroxyl groups of the ITO NPs and alkoxyl groups of MPS. Thus, compared to the pure ITO NPs, the size decreased as evidenced by the TEM measurements (Fig. 3). In order to test the stability, the ITO NPs were dispersed in HDDA via sonication and then mixed with

Fig. 4. Digital photographs of modified (a) and pure (b) ITO NPs dispersed in urethane acrylate oligomers.

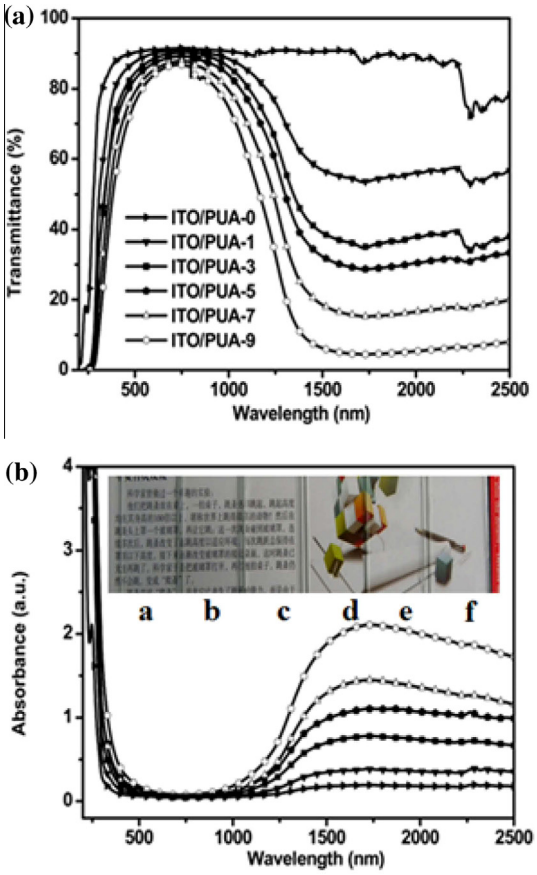

Fig. 5. UV–VIS–NIR spectra of ITO/PUA nanocomposites with different ITO contents (a) transmittance and (b) absorbance (the inset picture are digital photographs of 100 um thick ITO/PUA coatings on glass substrate containing 9 wt.%, 7 wt.%, 5 wt.%, 3 wt.%, 1 wt.% and 0 wt.% of the ITO NPS, respectively (A–F)).

urethane acrylate oligomers. The pure ITO NPs Fig. 4(b) finally sedimentated at the bottom of the container for less than one week and the modified ITO NPs Fig. 4(a) still retained homogeneous phase even for three months. The pure ITO NPs tend to form large particles and sedimentate quickly. While the modified ITO NPs showed good stability due to the steric hindrance of covalently grafting polymer chains of condensed MPS to the ITO NPs surfaces, and the polymer chains may modify the ITO surfaces, making them more hydrophobic, which is helpful to enhance the compatibility and long time stability. Furthermore, the small particle size of the modified ITO is favorable to minimize the light scattering, which is curial to fabricate high transparent nanocomposites.

3.2. Optical properties and morphology of ITO/PUA nanocomposite films

The transmittance and absorbance spectra of ITO nanocomposites containing various concentrations are shown in Fig. 5(a and b) respectively. The thickness of the obtained films coated on glass substrates was about 100 um. In the UV range, the neat PUA films only blocks UV light up to 250 nm. In other words, neat PUA are transparent for UVB (280–320 nm in wavelength) and UVA (320–400 nm in wavelength) irradiations that has degradation effects on various materials and detrimental effects to human health [1,8]. By introducing the ITO NPs into the polymer, UVB and UVA irradiations are efficiently filtered by the composite. Higher ITO loadings show stronger UV-shielding efficiency. For example, the transmittance of the coatings with 0 wt.%, 1 wt.%, 3 wt.%, 5 wt.%, 7 wt.% and 9 wt.% of the ITO nanoparticles at 350 nm in the UV region are 82%, 68%, 54%, 53%, 43% and 32%, respectively. In the UV range, as the ITO loadings increasing the absorption increases (Fig. 5(b)), which is in harmony with decreased transmission in the transmittance spectra. In the visible range (400–800 nm), the ITO/PUA coatings show good transparence with transmittances close to that of the neat PUA, except for that of high ITO concentrations which exhibit slightly decreased transmittance. The faint loss of transparency of nanocomposites owing to light scattering can explained by the Eq. (1) below.

$$T = \frac{I}{I_0} = \exp\left(-\left[\frac{3V_p\chi r^3}{4\lambda^4}\left(\frac{n_p}{n_m}-1\right)\right]\right) \quad (1)$$

where T is the transmittance of incident light, I and I_0 are the transmitted and incident light intensity, V_p is the volume fraction of inorganic particles, r is the radius of spherical particles, χ is the optical path length, λ is the wavelength of incident light, and n_p and n_m are the refractive index of nanoparticles and matrix [6,25]. Eq. (1) shows that the different refractive indexes of the filler ITO ($n \approx 1.9$) and PUA polymer matrix ($n \approx 1.6$) as well as relatively large particle of the agglomerated particle are responsible for reduction in the transmittance of nanocomposites in the visible range. In the NIR range Fig. 5(a), the neat PUA resin showed a constant more than 89% transmittance. The weak absorption peaks observed in the long IR range are assigned to the functional group absorption peaks of PUA coatings. With respect to the neat PUA coating, the ITO/PUA coatings show low transmittance in the NIR range. For example, the transmittance of the coatings with 0 wt.%, 1 wt.%, 3 wt.%, 5 wt.%, 7 wt.% and 9 wt.% of the ITO NPs at 1500 nm in the NIR region are 91%, 56%, 38%, 31%, 18% and 6%, respectively. Thus, the NIR transmission cutoff wavelength of the ITO/PUA coatings shifts to shorter wavelength with increasing content of ITO NPs.

As shown in the inset digital photographs of Fig. 5(b), the composite coatings show high clarity and no visible lump was observed for all the samples. The interesting optical properties of the nanocomposites suggest a good dispersion of the ITO NPs in the PUA matrix. This can be proved by scanning electron microscopy (SEM) images of the cross-sectional fractured surface of the composites coatings. Fig. 6(a and b) shows the images of neat PUA ma-

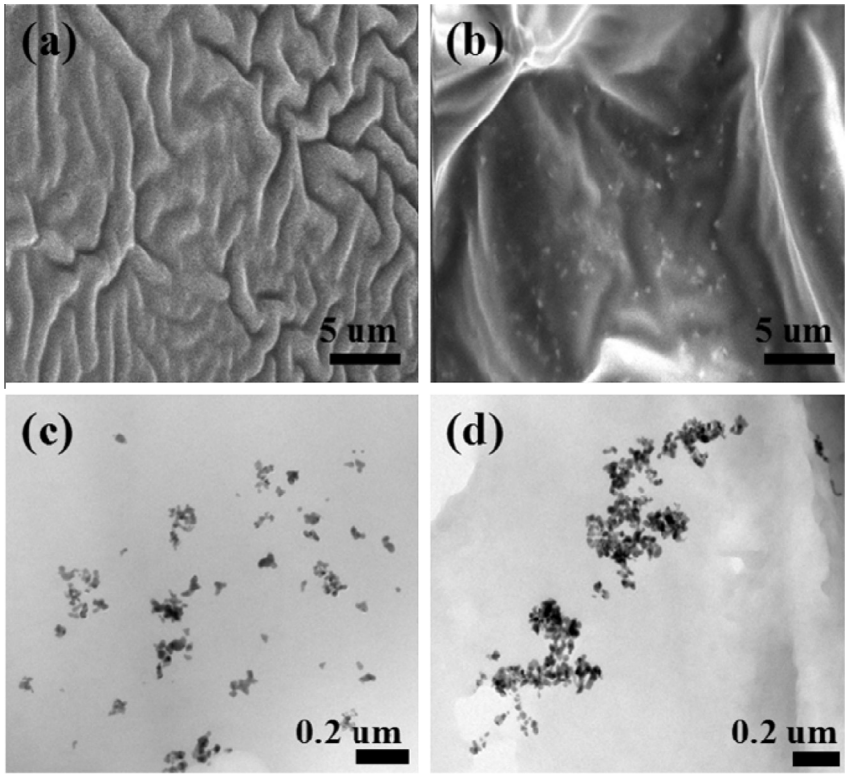

Fig. 6. SEM images of the cross-sectional fractured surface of the composites coatings ((a) ITO/PUA-0, (b) ITO/PUA-7) and TEM images of the cross-section of the composite coatings ((c) ITO/PUA-9 and (d) ITO/PUA-9 with pure ITO NPs).

trix and nanocomposites filled with 7 wt.% ITO, respectively. Compared to the PUA coatings, the distribution of the ITO can be easily identified. The ITO NPs appear as white dots, whose concentration on the fracture surface of the nanocomposites increases as the filler loading increasing. It can be seen that the ITO NPs are homogeneously dispersed in the matrix and no large agglomerates were observed. The dispersion state of ITO NPs in the PUA matrix is significantly different from that of nanocomposites prepared by the simple blending the PUA and pure ITO NPs. Fig. 6(c) and (d) shows the TEM images of ITO/PUA nanocomposite with modified and pure ITO NPs (9 wt.%). From the TEM images, it can be seen that the modified ITO NPs were well dispersed in the polymer matrix while the pure ITO NPs were aggregated severely in the polymer matrix with the larger particle size. The optical properties and digital photographs of the ITO/PUA nanocomposite with pure ITO (9 wt.%) and modified ITO (9 wt.%) NPs are shown in Fig. 7. It is evident that the former shows less transparent in the visible range with respect to the modified ITO/PUA nanocomposite. It can be concluded that grafted ITO NPs in the PUA matrix are beneficial for the minimization of the aggregation of NPs and homogeneous dispersion in the matrix. Additionally, the chemical similarity of the grafted polymer chains of ITO NPs with the matrix reduce the mixing enthalpy,which is responsible for the stabilization of ITO/PUA solution for several months and enhanced compatibility between the fillers and matrix. Therefore, in order to obtain high transparent ITO/PUA nanocomposites, the modification of ITO is important to lower the scattering loss.

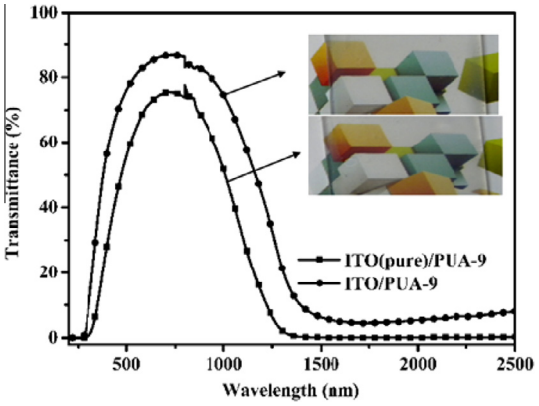

Fig. 7. UV–VIS–NIR spectra of ITO/PUA-9 and ITO/PUA-9 with pure ITO NPs (the inset picture are digital photographs of 100 um thick ITO/PUA coatings on glass substrate).

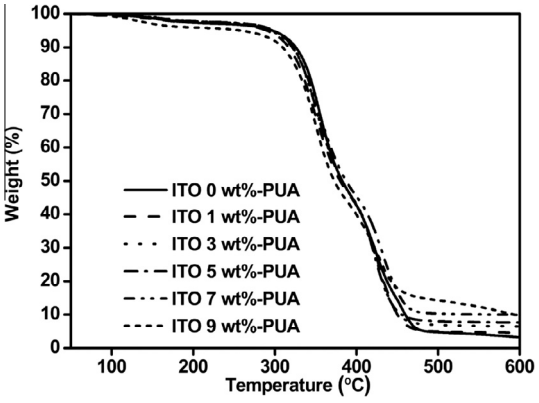

Fig. 8. TGA curves of ITO/PUA nanocomposites.

3.3. Thermal properties of ITO/PUA nanocomposites

It is generally believed that the incorporation of inorganic fillers into polymers can reinforce thermal stability because of physical confinement and interactions between the polymer chains and the filler surface [18,26,27]. To investigate how ITO NPs impact the thermal stability of the ITO/PUA nanocomposites, TGA analyses were performed in a nitrogen atmosphere. The TGA curves are shown in Fig. 8. It is noteworthy that compared with the pure PUA, the ITO incorporated composites showed no obvious enhancement of thermal stability. In contrast, ITO/PUA nanocomposites with high ITO contents exhibit lower onset decomposition temperatures. The decrease in thermal stability can be attributed to the strong absorption of UV radiation of ITO NPs which lead to the incomplete curing of the UV-cured ITO/PUA nanocomposites. Though, under the experimental conditions of our research, the surfaces of ITO/PUA nanocomposites are all tack-free, further work will be done to raise the curing degree and thermal stability.

4. Conclusions

In this work, highly transparent ITO/PUA nanocomposite coatings had been fabricated by incorporating 3-(trimethoxysilyl)propylmethacrylate (MPS) modified ITO NPs into a transparent UV curable urethane acrylate resin. The FTIR and TGA result confirmed that the MPS was grafted to the surface of ITO NPs successfully. Owing to the surface modification, the ITO NPs were able to uniformly dispersed in the PUA matrix. The composite coatings possess appealing optical properties: UVB (280–320 nm in wavelength) and UVA (320–400 nm in wavelength) irradiations are efficiently filtered by the composite films, and the prepared ITO/PUA nanocomposites show high transparency of visible light close to neat PUA resin and low transmittance of near-infrared (NIR) light. Increasing the ITO concentration gives rise to higher NIR shielding efficiency. Thus, the ITO/PUA composites can be easily adopted in industrial production to behave as functional optical coatings of glass and other substrates.

Acknowledgement

The authors are grateful to the support of National Natural Science Foundation of China (No. 51103160).

References

[1] Tu Y, Zhou L, Jin YZ, Gao C, Ye ZZ, Yang YF, et al. Transparent and flexible thin films of ZnO–polystyrene nanocomposite for UV-shielding applications. J Mater Chem 2010;20(8):1594–9.
[2] Koziej D, Fischer F, Kraenzlin N, Caseri WR, Niederberger M. Nonaqueous TiO_2 nanoparticle synthesis: a versatile basis for the fabrication of self-supporting, transparent, and UV-absorbing composite films. ACS Appl Mater Interf 2009;1(5):1097–104.
[3] Zeng X-F, Kong X-R, Ge J-L, Liu H-T, Gao C, Shen Z-G, et al. Effective solution mixing method to fabricate highly transparent and optical functional organic–inorganic nanocomposite film. Ind Eng Chem Res 2011;50(6):3253–8.
[4] Yin Y, Zhou S, Gu G, Wu L. Preparation and properties of UV-curable polymer/nanosized indium-doped tin oxide (ITO) nanocomposite coatings. J Mater Sci 2007;42(15):5959–63.
[5] Liu H, Zeng X, Kong X, Bian S, Chen J. A simple two-step method to fabricate highly transparent ITO/polymer nanocomposite films. Appl Surf Sci 2012;258(22):8564–9.
[6] Philosophical Magazine A, Tao P, Viswanath A, Schadler LS, Benicewicz BC, Siegel RW. Preparation and optical properties of indium tin oxide/epoxy nanocomposites with polyglycidyl methacrylate grafted nanoparticles. Acs Appl Mater Interf 2011;3(9):3638–45.
[7] Miyazaki H, Ota T, Yasui I. Design of ITO/transparent resin optically selective transparent composite. Sol Energy Mater Sol Cells 2003;79(1):51–5.
[8] Luo Y-S, Yang J-P, Dai X-J, Yang Y, Fu S-Y. Preparation and optical properties of novel transparent al-doped-ZnO/epoxy nanocomposites. J Phys Chem C 2009;113(21):9406–11.

[9] Sun J, Gerberich WW, Francis LF. Electrical and optical properties of ceramic–polymer nanocomposite coatings. J Polym Sci, Part B: Polym Phys 2003;41(14):1744–61.
[10] Wouters MEL, Wolfs DP, van der Linde MC, Hovens JHP, Tinnemans AHA. Transparent UV curable antistatic hybrid coatings on polycarbonate prepared by the sol–gel method. Prog Org Coat 2004;51(4):312–20.
[11] Zhou S, Wu L. Phase separation and properties of UV-curable polyurethane/zirconia nanocomposite coatings. Macromol Chem Phys 2008;209(11):1170–81.
[12] Redel E, Huai C, Dag O, Petrov S, O'Brien PG, Helander MG, et al. From bare metal powders to colloidally stable TCO dispersions and transparent nanoporous conducting metal oxide thin films. Small 2012;8(24):3806–9.
[13] Li J, Wang L, Liu J, Evmenenko G, Dutta P, Marks TJ. Characterization of transparent conducting oxide surfaces using self-assembled electroactive monolayers. Langmuir 2008;24(11):5755–65.
[14] Sunde TOL, Garskaite E, Otter B, Fossheim HE, Saeterli R, Holmestad R, et al. Transparent and conducting ITO thin films by spin coating of an aqueous precursor solution. J Mater Chem 2012;22(31):15740–9.
[15] Sasaki T, Endo Y, Nakaya M, Kanie K, Nagatomi A, Tanoue K, et al. One-step solvothermal synthesis of cubic-shaped ITO nanoparticles precisely controlled in size and shape and their electrical resistivity. J Mater Chem 2010;20(37):8153–7.
[16] Hong L, Paramonov P, Bredas JL. Theoretical study of the surface modification of indium tin oxide with trifluorophenyl phosphonic acid molecules: impact of coverage density and binding geometry. J Mater Chem 2010;20(13):2630–7.
[17] Kim BK, Cho YH, Lee JS. Effect of polymer structure on the morphology and electro-optic properties of UV curable PNLCs. Polymer 2000;41(4):1325–35.
[18] Lee SK, Yoon SH, Chung I, Hartwig A, Kim BK. Waterborne polyurethane nanocomposites having shape memory effects. J Polym Sci, Part A: Polym Chem 2011;49(3):634–41.
[19] Kim D, Jang M, Seo J, Nam K-H, Han H, Khan SB. UV-cured poly(urethane acrylate) composite films containing surface-modified tetrapod ZnO whiskers. Compos Sci Technol 2013;75:84–92.
[20] Capozzi CJ, Gerhardt RA. Novel percolation mechanism in PMMA matrix composites containing segregated ITO nanowire networks. Adv Funct Mater 2007;17(14):2515–21.
[21] Wakabayashi A, Sasakawa Y, Dobashi T, Yamamoto T. Optically transparent conductive network formation induced by solvent evaporation from tin-oxide-nanoparticle suspensions. Langmuir 2007;23(15):7990–4.
[22] Luo XT, Han JS, Ning Y, Lin Z, Zhang H, Yang B. Polyurethane-based bulk nanocomposites from 1-thioglycerol-stabilized CdTe quantum dots with enhanced luminescence. J Mater Chem 2011;21(18):6569–75.
[23] Bressy C, Van Giang N, Ziarelli F, Margaillan A. New insights into the adsorption of 3-(trimethoxysilyl)propylmethacrylate on hydroxylated ZnO nanopowders. Langmuir 2012;28(6):3290–7.
[24] Kim D, Jeon K, Lee Y, Seo J, Seo K, Han H, et al. Preparation and characterization of UV-cured polyurethane acrylate/ZnO nanocomposite films based on surface modified ZnO. Prog Org Coat 2012;74(3):435–42.
[25] Yang Y, Li Y-Q, Fu S-Y, Xiao H-M. Transparent and light-emitting epoxy nanocomposites containing ZnO quantum dots as encapsulating materials for solid state lighting. J Phys Chem C 2008;112(28):10553–8.
[26] Sun D, Miyatake N, Sue H-J. Transparent PMMA/ZnO nanocomposite films based on colloidal ZnO quantum dots. Nanotechnology 2007;18(21).
[27] Uhl FM, Davuluri SP, Wong SC, Webster DC. Organically modified montmorillonites in UV curable urethane acrylate films. Polymer 2004;45(18):6175–87.